Developing a Non-linear Fractional Order Model for Lithium-ion Batteries Considering the Affecting Factors

Ali Moshar Movahhed[1,*], and Seyed Kamal Hosseini Sani1

[1] *Electrical engineering department, Engineering faculty, Ferdowsi university of Mashhad, Mashhad, Iran*
**Corresponding author: k.hosseini@um.ac.ir*

Manuscript received 11 October 2024; revised 03 January, 2025; accepted 21 January, 2025. Paper no. JEMT-2410-1530.

The growing applications of lithium-ion batteries worldwide demonstrate the importance of accurate estimation of the state of charge (SOC) of batteries, as this directly impact charging quality and battery performance, and serves as a key indicator for users. Despite the importance of SOC, there is no physical device to measure it from the battery terminal. This paper proposes a comprehensive nonlinear fractional order model incorporating key factors affecting SOC estimation such as battery hysteresis effect, temperature, and age of battery into the model structure. In order to acquire thorough and broad range of experimental data, a battery tester and a data logger were set up through gathering the data under different conditions over a substantial period of time. The electrical elements of the equivalent circuit model were obtained using a PSO algorithm, and then input into the state-space equations. Based on the model outputs, a look-up table was generated for various conditions. Being reasonably accurate, the table could reduce intensive calculations considerably. Proposed nonlinear fractional order model, significantly reduces the computational overhead compared to adaptive models. Therefor by considering the electrical parameters as constant values and transferring all non-linearity and changes such as hysteresis effect, temperature and life cycle of studied battery in VOC function, the experimental results confirm the accuracy of proposed model.

Keywords: *State of charge (SOC), Battery hysteresis, Equivalent electrical circuit, Lithium-ion batteries, Electrical vehicle*.

http://dx.doi.org/10.22109/jemt.2025.482452.1530

1. Introduction

With the recent rapid expansion of smart grids and use of electric vehicles and new energies, batteries have emerged as the most important source of energy storage. Meanwhile, lithium batteries are used as a reliable and easy-to-use source for electrifying cars and storing energy electrochemically. Accurate and reliable estimation of state of charge (SOC) is a major challenge in the industry[1]. To determine the general conditions of the batteries, parameters such as SOC, depth of discharge and state of health (SOH) are considered important. Having exact values of SOC in various applications is very crucial, and no physical devices have so far been developed to measure these parameters[2]. There are various methods for estimating SOC based on external parameters like voltage and current. One way is a measure the battery terminal voltage. It is clear that the amount of voltage measured at the battery terminal will vary in the presence of current and will vary according to the load on the battery output. Therefore, it is not possible to determine SOC instantly and accurately simply by measuring the output voltage of the battery. The Columbine counting method or ampere- hour counting is another practical method that has been proposed and used in practice. In load counting method, there is a considerable deal of dependence on the initial conditions. This means that the amount of initial stored load is important because estimating the amount of battery charge at any later time is based on initial amount. Precise estimation of SOC is not only for use in the battery management system, which leads to increasing the quality of charge, but also to protect the battery from overcharging or deep discharge in order to extend the overall battery lifespan. Existing methods of battery SOC estimation are either not accurate enough or impractical due to their high complexity[3]. In order to estimate the state of health (SOH) and SOC of lithium-ion batteries, a hybrid approach, based on multi-layer perceptron (MLP) with extreme gradient boosting (XGBoost) algorithm is proposed in[4]. Two RC equivalent circuit models of lithium-ion batteries are developed and used in[5].

It is obvious that development of a precise mathematical model is the first step of accurate control and stability of a system. The main idea of modeling a battery and achieving internal state variables, including SOC is based on measurable signals such as battery voltage and battery output current. In general, three different models are used to model batteries: 1) electrochemical model, 2) electrical model, and 3) fuzzy model[6]. In mathematical modeling of batteries, the use of equivalent electrical model is very common[7-9]. One of the disadvantages of this model is its inability to exactly model the current electrochemical process in the battery because it only describes the input and output behavior based on electrical elements. The use of electrochemical models through partial equations will help solving some problems of equivalent electrical circuit models. Although they describe the phenomenon of ion transfer and electrochemical reactions using partial equations more accurately, but the number of calculations will be too heavy. Even with the simplest electrochemical models like

single-particle model, 10 unknown parameters for designing estimates of battery SOC will be required, which indicates a high computational volume in these models[10].

A fractional-order hysteresis equivalent circuit model is used and electrical parameters are identified by PSO algorithm which optimized by genetic algorithm, and a fractional order adaptive unscented Kalman filter is drived to estimate SOC of lithium-ion batteries[11].

In [12] a multi layered long short-term memory (MLLSTM) is proposed. by measuring voltage and current, parameters of the battery is identified using an adaptive multi time-scale identification strategy (AMIS) with frequency feature decomposition.

A new adaptive genetic algorithm (AGA) is proposed to estimate SOC of lithium0ion batteries by considering temperature affects on prediction performance. Finally, combination AGA and adaptive unscented Kalman Filter (AUKF) is proposed and employed to estimate SOC[13].

Improved adaptive extended Kalman filter (IAEKF) is employed to estimate SOC of lithium-ion batteies precisely. Hence, experimental results confirm that IAEKF in comparison to other AEKF algorithm achieves better estimation accuracy and robustness [14].

The main objective of this research is to develop a method for estimating SOC of lithium-ion batteries as a critical parameter, with relatively low computational complexity and high accuracy. This method aims to account for factors such as hysteresis effects, temperature, and battery aging, making it suitable for practical applications.

2. Basic Definition

In order to describe and analyze the performance of batteries to achieve an equivalent and appropriate model that can be used to simulate the dynamic behavior of the battery and extract the desired parameters like SOC, it is necessary to introduce backgrounds in this area. In the following, some types of batteries which is one of the most common and widely used methods of energy storage, are briefly introduced. Given the expansion of the use of fractional calculus in the control and definition of practical applications is presented [15, 16].

2.1. Energy Storage System

Storage systems as one of the most important components of electric vehicles and grid-independent power supply systems have various types, including mechanical, chemical, electrochemical, electrical and heating; among them electrochemical methods (conventional batteries) particularly have been growing rapidly in recent years. In general, every battery's structure consists of cells, each responsible for providing part of the required power in which, a reversible conversion between electrical and chemical energy in charge and discharge process that is the fundamental principle behind the operation of electrochemical batteries allows for the storage and release of energy as needed. These battery cells are connected in series, which creates a cumulative voltage across the entire series that provides voltage demand to meet the requirements of the applications. Also, to provide sufficient current, the battery packs are created by connecting the modules in parallel. Moreover, batteries are different by such features, specifically mass and energy density, which are decisive when choosing a battery for electric vehicles, so that lower mass and higher energy destiny are desired. Nickel-cadmium and nickel-metal hydride batteries were used in the first generation of portable electronics and quickly became popular due to their small size and greater energy storage. Larger dimensions of these batteries were in electric vehicles used for higher energy density and lower mass comparing to lead-acid batteries. However, due to the toxicity of cadmium, shorter life and lower energy density of Nickel-cadmium batteries, they are being replaced by nickel-metal hydride batteries. Despite the advantages of nickel-metal hydride batteries, because of the high rate of spontaneous discharge, lithium-ion batteries have become a dominant technology in modern portable electronics and electric mobility applications thanks to their high energy density, high electrochemical potential, rechargeability, low self-discharge rate, lack of memory effect, low weight, longer life, and environmentally friendly features[17, 18]. Nowadays, different types of lithium-ion batteries with differences in cathode, anode and electrolyte are designed and manufactured to increase the lifespan and safety and reduce the cost of raw materials. A comparison between several types of batteries based on power density and energy is given in Fig. 1.

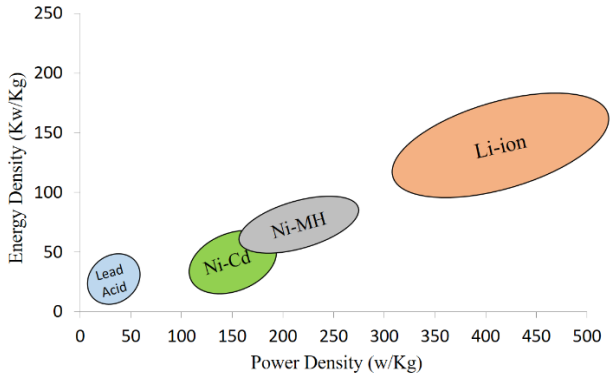

Fig. 1. Comparison of several types of batteries

Other types of lithium batteries include lithium-ion polymer as a new generation of high-performance lithium batteries, lithium-manganese and lithium-titanite[19].

2.2. Battery Management System

Along with the increasing growth of batteries applications in electric vehicles, smart grids and renewable energy systems, battery management system (BMS) is overstated in terms of providing safety, prolonged battery life, efficient energy management, performance optimization and data logging and diagnostics in which SOC and SOH represent the available capacity of the battery and the overall capability of the battery relative to its original, respectively[20]. BMS is one of the essential parts which is used in battery-based systems. One major input to BMS is SOC; therefore, SOC estimation plays a crucial role in battery modelling and BMS[21].

A comprehensive BMS should have all the features, including protection and safety of the battery against various environmental factors such as overcharging or deep discharge, management and control of battery temperature, monitoring of battery cells, balance and battery data collection. Although the discharge current of the battery depends on the output load, which is located in the output of the battery and varies according to the type of application, the charge rate must follow certain standards to perform the charging operation with the highest efficiency and the least damage to the battery[22]. Another important environmental factor is the issue of temperature management because its increase can increase the resistance inside the battery, and thus, reduces the energy capacity stored in the battery. Therefore, one of the tasks of the battery management system will be to monitor and control the battery temperature under various operating conditions and adjust it within the permissible range[23]. The battery charge estimate actually represents the available energy stored related

to the total battery capacity shown in Fig. 2 [24].

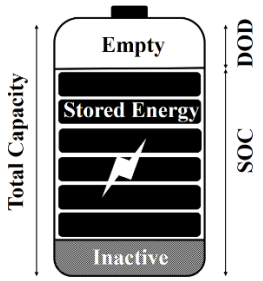

Fig. 2. Graphical view of total battery capacity

Despite the importance of SOC, there is no physical device to measure it from the battery terminal. Existing methods for measuring battery SOC that are used in practice do not have sufficient accuracy and are not easily applicable to methods that have high accuracy and online estimation[25].

Amper hour approach is the most common and practical method in this case:

$$S(t) = S(t_0) - \frac{1}{Q}\int_{t_0}^{t} \eta i(t) dt \quad \textbf{(1)}$$

Where, S(t0) denotes the initial value of SOC at t0, S(t) displays SOC at time t. η is charging/discharging efficiency, and i(t) is battery's instantaneous charging or discharging current[21].

2.3. Hysteresis Effect

Research findings show that VOC-SOC relation is not a one-to-one mapping function (Fig. 3). In the same charge condition, the battery is in different discharge situation. The effect of hysteresis on lithium batteries is due to the effect of thermodynamic entropy, mechanical stress, and microscopic deformation inside the active electrode components during lithium adsorption and extraction.

The magnification clearly indicates that the path of battery charge is different from the path of battery return or discharge; this issue (if not taken into account seriously) may cause errors in the modeling and correct identification of the battery. One simple way to model hysteresis effect is to extract two different functions and a reference table for the battery charge and discharge curve[26].

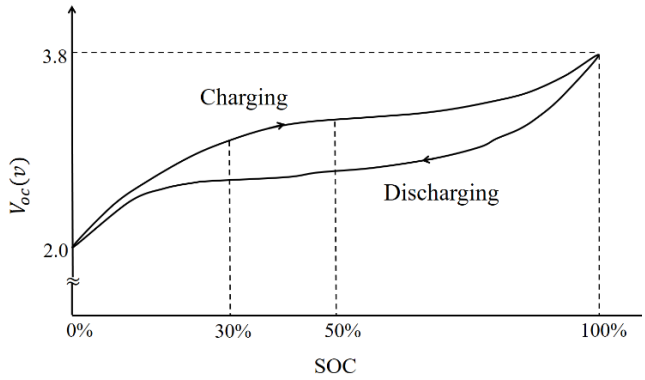

Fig. 3. Hysteresis effect in batteries

2.4. Fractional Calculus

Over the last two decades, the application of fractional control has spread out due to its robust performance. There exist some definitions for fractional calculus[27, 28].

Rieman-Liouville fractional order integral is defined as follows:

$$I_c^{\alpha} F(t) \overset{\Delta}{=} \frac{1}{\Gamma(\alpha)}\int_c^t (t-\tau)^{\alpha-1} f(\tau) d\tau \qquad t > c\ ,\ \alpha \in R^+ \quad (1)$$

Where, Γ is the Gamma function.

Note that substituting by in order to reach fractional order differential operator is impossible.

Rieman-Liouville definition for the fractional order derivative of has the following form[29]:

$$ {}_R^{\alpha}D^{\alpha} f(t) \triangleq D^m I^{m-\alpha} f(t) \quad (2)$$
$$= \frac{d^m}{dt^m}\left[\frac{1}{\Gamma(m-\alpha)}\int_0^t \frac{f(\tau)}{(t-\tau)^{\alpha-m-1}} d\tau\right]$$

Where, $m-1\langle\alpha\langle m, m \in N$

Another definition was introduced by Caputo as Eq. (3)[30]:

$$ {}_c^{\alpha}D^{\alpha} f(t) \triangleq I^{m-\alpha} D^m f(t) = \frac{1}{\Gamma(m-\alpha)}\int_0^t \frac{f^{(m)}(\tau)}{(t-\tau)^{\alpha-m+1}} d\tau \quad (4)$$

Where, $m-1\langle\alpha\langle m, m \in N$

Laplace transform is the next operator, which is used in this paper. It is given for Caputo fractional order derivative as Eq. (5) [31]:

$$\ell\left[{}_c^{\alpha}D^{\alpha} f(t)\right] = s^{\alpha} F(s) - \sum_{k=0}^{m-1} s^{\alpha-k-1} f^{(k)}(0) \quad 5)$$

It is worth noting that due to the expansion of fractional order calculus in engineering during a couple of decades and also the growth of fractional order control in this area, only brief explanations have been provided.

3. Battery Identification

There are various identification methods to determine and specify the unknown parameters of the system fractional order model; we used the battery system in this study. The method presented in [23] has a good performance, but due to the high computational volume, including convolution operations, it takes up a lot of time. Although replacing the indirect detection method with discrete time model parameters can solve the problems mentioned above, rapid dynamics may be lost during the sampling process. However, relatively small sampling times will lead to numerical problems that limit identification of unknown parameters in the discrete time model [32]. In addition, identifying model parameters can be sensitive to initial conditions and noise and limit real-time applications. In this process, because these batteries have both fast and slow dynamics, the choice of sampling time must be done very carefully [33]. One of the identification methods in nonlinear systems along with neural network and Volta series method is Wiener-Hammerstein method. In comparison, there is a nonlinear system in nonlinear methods and

identification is done using existing methods. In [34], to overcome the problems of discrete time method, continuous time system identification is used because it creates a good view of the system features and prevents data from being ignored due to high sensitivity to the factors. In [35], continuous time system identification is compared with indirect identification of discrete time system in battery applications [36]. The method proposed in this proposal is to simplify the problem from a complex nonlinear system to a linear system under special conditions [37], i.e. keeping the SOC and all environmental factors constant. In this way, the amounts of terminal voltage and open circuit voltage are measured. For example, a current of 1 ampere is taken from the battery for a few seconds under standard conditions, and after a long time and when all the dynamics are damped, the amount of terminal voltage, which is the same as the open circuit voltage, is recorded. In the next step, by collecting data and clustering them, the function of the relationship between open circuit voltage and battery charge status is calculated by considering the temperature and operating mode, i.e. charging or discharging mode [38].

3.1. Data Acquisition

In order to collect real time and true data of battery charge and discharge, including battery current, terminal voltage, temperature and SOC, a data logger based on digital and analogue sensors was designed and established. SOC was measured by ampere-hour counting approach and validated by physically measuring the amount of charge.

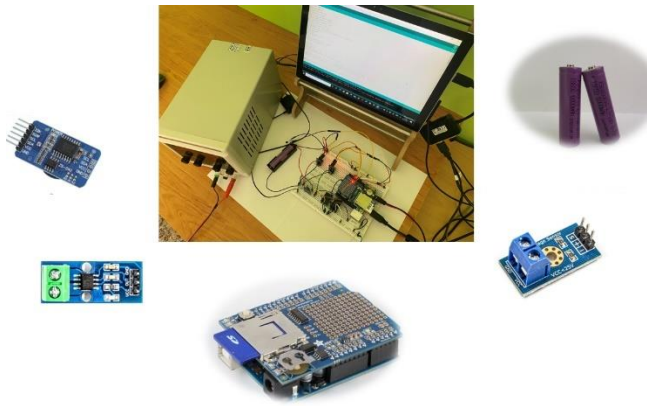

Fig. 4. Data logger for battery tests

To collect battery data, a data logger was designed so that one Arduino UNO (as a microcontroller), ACS712 current measurement sensor, SD card and its module, DS3231 clock module, digital temperature measurement module, TP4056 charging and discharging lithium-ion batteries module and a voltage measurement module were used. Finally, by applying various conditions, all parameters and environmental situation during extensive time span were saved.

3.2. Battery Discharging

The assembled data logger was applied to a lithium-ion battery with the characteristics listed in Table 1.

Table 1. Battery characteristics

Voltage (v)	Capacity (mAh)	Size	Type
1.5	2000	19650	Li-ion

In this stage, the battery was tested and examined by applying a resistive load in the form of pulses with the width of approximately 10 minutes and rest periods of more than one hour.

Battery current versus terminal voltage values is shown in Figs. 5 and 6, respectively.

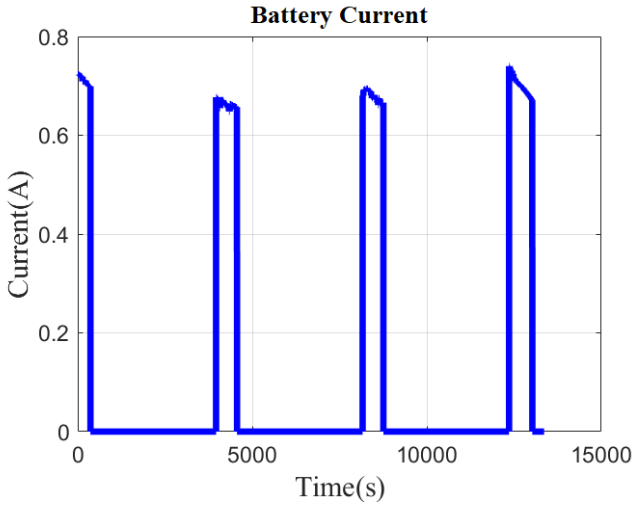

Fig. 5. Measured discharging current of battery

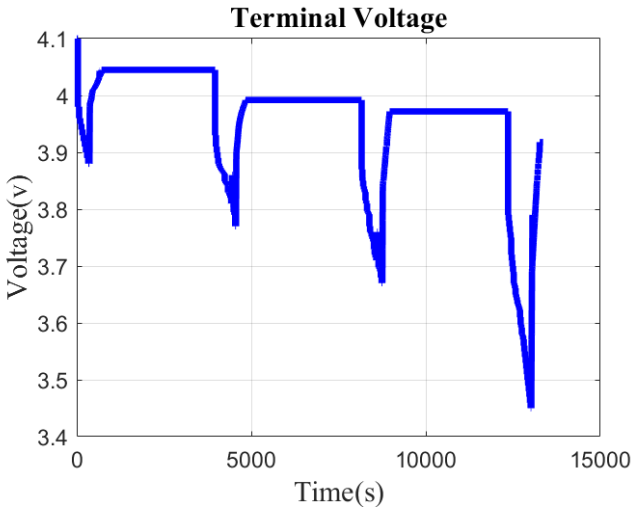

Fig. 6. Measured discharging voltage of battery

Another challenging parameter that plays an important role in estimating SOC is the OCV of battery. Since it is not possible to access this parameter directly, then in order to collect this parameter, it is assumed that the real value of OCV is equal to terminal voltage after 1 or 2 hours of resting and settling down of the transient condition. It means that after each test on battery, it was given approximately 2 hours of rest time before the next round; this allows the battery to stabilize in terms of overheating, chemical reactions, and the transient voltage output dissipation so the terminal voltage becomes equal to the OCV. Applying this procedure leads to gather the OCV of the battery.

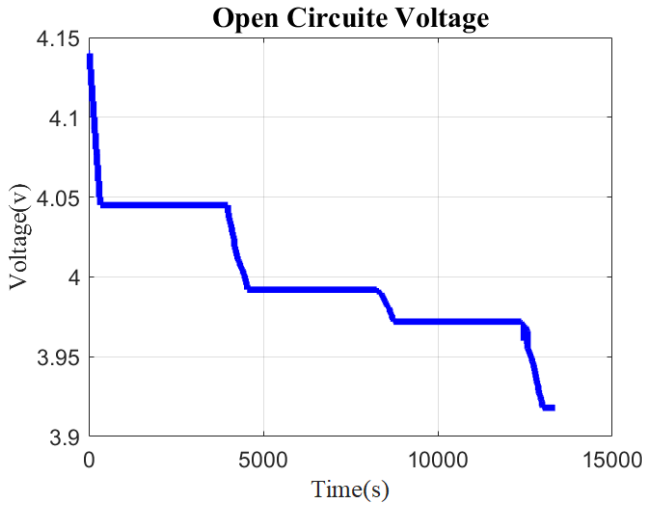

Fig.7. Extracted OCV of battery

The hysteresis effect, presented in Fig. 8 based on the collected data and plotting of OCV as a function of battery SOC, was measured using the Coulomb counting algorithm.

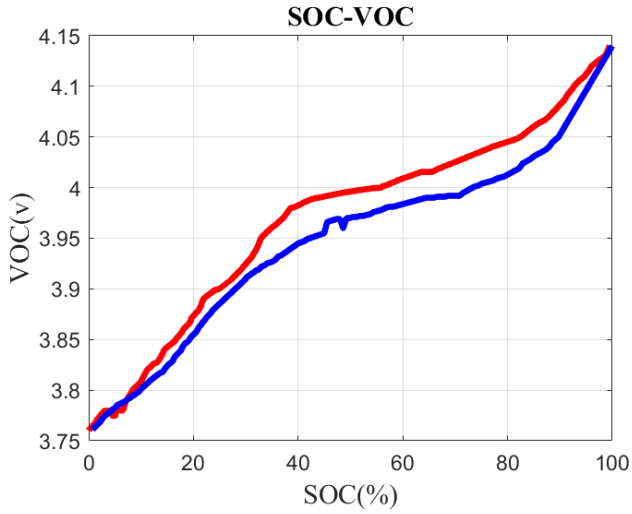

Fig. 8. Hysteresis effect on the studied battery

As clearly shown in Fig. 8, the presence of a hysteresis effect results in a noticeable difference between the charge and discharge curves of the battery's OCV, which has significant implications for battery modeling and SOC estimation. Proper calculation of the hysteresis effect can avoid considerable errors that would affect the modelling of battery behavior.

3.3. New Battery Discharging

In this research, two main tests were conducted on the battery, which capture all the battery dynamics to provide more accurate information for modelling the battery. In the previous step, data related to the used battery and measurements were conducted in a discontinuous manner with time intervals between them for the rest of the battery operation. Then all the tests were conducted frequently without any rest time in order to monitor the voltage until reaching an unused range, which is about 3.3V particularly in this case, considering SOC to be zero. The battery current in the presence of constant resistive load at battery output is shown in Fig. 9.

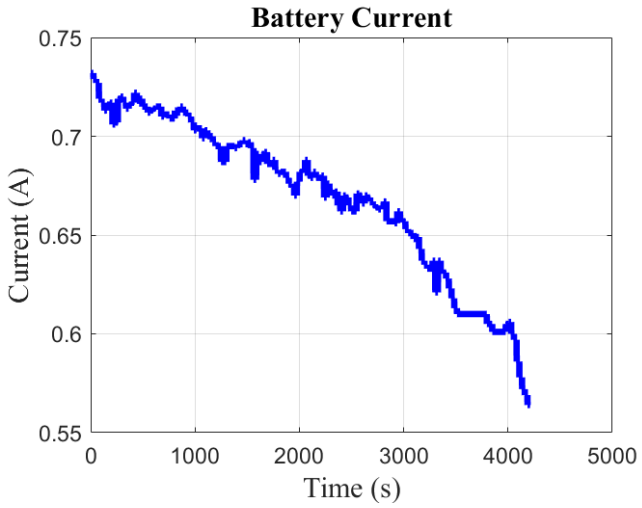

Fig. 9. Measured discharging current of new battery

The measured battery terminal voltage in continuous discharging state is illustrated in Fig. 10.

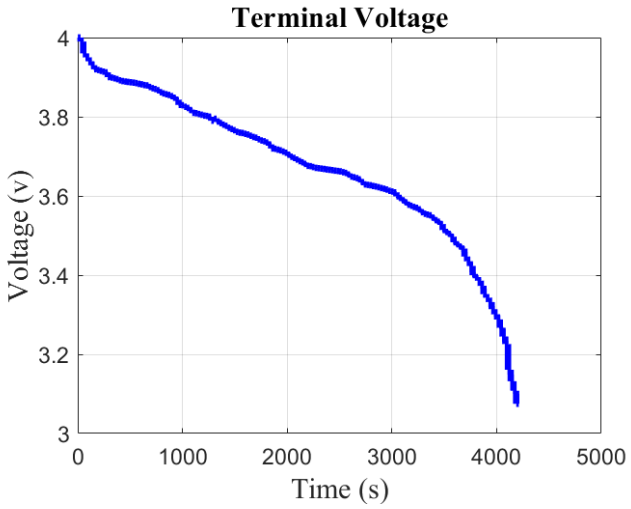

Fig. 10. Measured discharging voltage of battery

As mentioned earlier, the OCV could be obtained under specific conditions. The changes in the OCV voltage of new battery in continuous discharging state are displayed in Fig. 11.

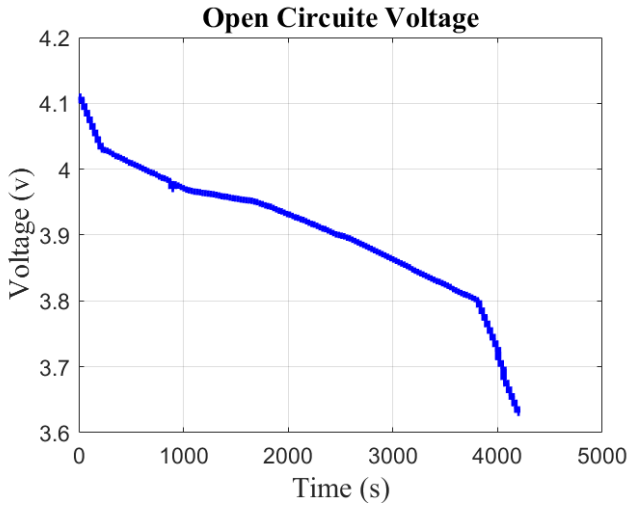

Fig. 11. Extracted OCV of battery

Fig. 12 presents the hysteresis effect based on the data collected for the new battery.

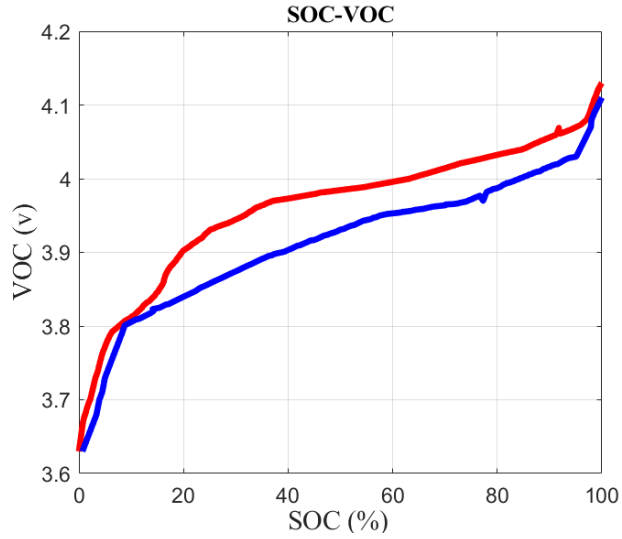

Fig. 12. Hysteresis effect on the new battery

Considering the large number of tests and data acquisition, only some of the figures are presented in this research and the rest were used for modeling and determining the nonlinear fractional order state space model of battery.

4. Battery Modelling

In electrical models, the required parameters are changed by changing the charge and discharge rate, SOC, temperature and ageing level; therefore, they must be identified and updated online [39].

In this research, battery parameters were assumed constant parameters as identified by the manufacturer. On the other side, unlike commonly known methods of integer order, fractional order derivatives allow an explanation of matter transfer, diffusion, and memory in dielectrics [40]. In batteries, especially lithium-ion type, fractional order differential system is used to describe the electrical dynamics, including material and charge transfer process in the electrolyte, and material diffusion and porosity in solid electrodes [41, 42].

4.1. Equivalent Electrical Circuit Model

First, a first-order equivalent electrical circuit model (Fig. 13) was chosen to identify the accuracy of parameters by writing the description equations and applying the PSO algorithm. It was found that this model does not have sufficient accuracy, so a second-order equivalent electrical circuit model (Fig. 14) was replaced [43].

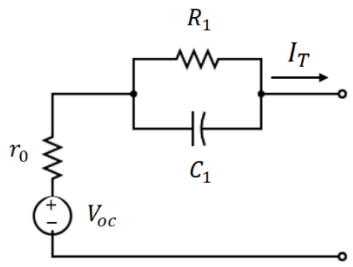

Fig. 13. First-order equivalent electrical circuit model

The first-order and second-order models have been extensively used in various researches. The findings have shown that increasing the number of RC branches does not lead to a significant improvement in accuracy; rather it increases the model complexity. As a result, in this case, the second-order model was used as a trade-off between computational load and model accuracy.

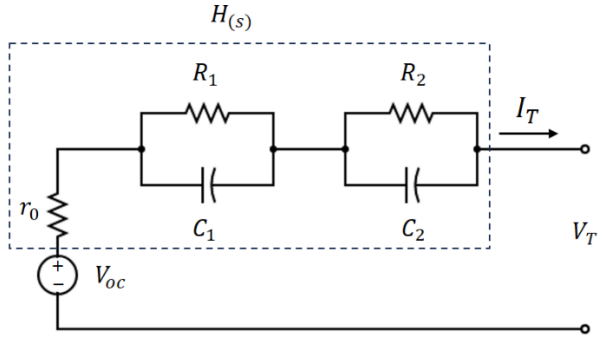

Fig. 14. Second-order equivalent electrical circuit model

To determine the value of parameters R_0, R_1, R_2,C_1,C_2, alpha and beta based on the measurements of V_{OC}, V_T and I_T, a linear transfer function, H(s), is defined as Eqs. 6 and 7:

$$H(s)=\frac{V_O(s)}{I_T} \tag{6}$$

$$H(s)=\frac{a_1 s^{(\alpha+\beta)}+b_1 s^{\alpha}+c_1 s^{\beta}+d_1}{a_2 s^{(\alpha+\beta)}+b_2 s^{\alpha}+c_2 s^{\beta}+d_2} \tag{7}$$

$$\begin{Bmatrix} a_1=R_0R_1R_2C_1C_2 \\ b_1=R_1C_1(R_0+R_2) \\ c_1=R_2C_2(R_0+R_1) \\ d_1=R_0+R_1+R_2 \end{Bmatrix}, \begin{Bmatrix} a_2=R_1R_2C_1C_2 \\ b_2=R_1C_1 \\ c_2=R_2C_2 \\ d_2=1 \end{Bmatrix} \tag{8}$$

Where, $V_O=V_{OC}-V_T$.

In order to omit the nonlinearity part of the equivalent electrical circuit model of the battery, H(s) is considered as a linear transfer

function. The unknown parameters of H(s) are identified and implemented in nonlinear state space model through performing various simulations and experiments.

The voltage of H(s) (in Fig. 15 shown by dashed line in Fig. 14)) in Fig. 15 for used battery with non-continuous discharging algorithm is presented in Fig. 15 as transfer function voltage.

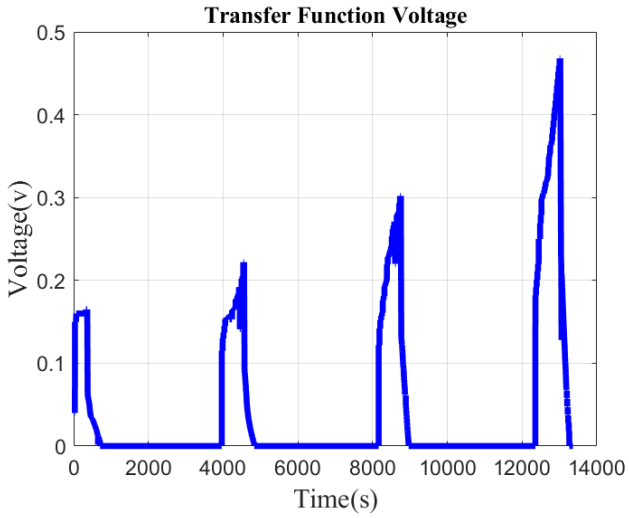

Fig. 15. Voltage of H(s) in piecewise discharging of used battery

Various experiments have been carried out to identify the unknown parameters, and the curve of continuous discharging of used battery is shown in Fig. 16

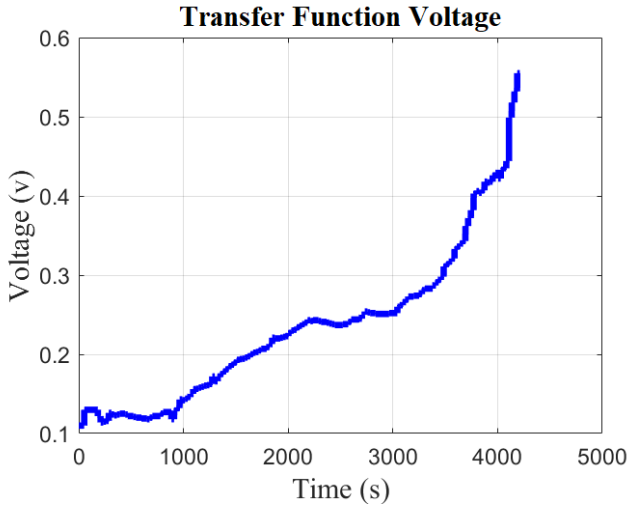

Fig. 16. Voltage of H(s) in continues discharging of new battery

4.2. Determining Parameters

Unknown parameters where determined based on our prior knowledge modelling of electrochemical process follows fractional equations. Technically speaking, the parameters such as resistors and capacitors are not constant values due to electrochemical process inside of battery. Therefore, in this research electrical elements and fractional order degrees assumed as constant values based on H(s) linear model. Then they were considered within nonlinear terms in the state space model. It is notable that one of the most important variables in exact modeling of battery is the relation between the battery's OCV and SOC, which is determined in next section.

To determine the electrical model parameters, the PSO algorithm was implemented with the input data I_T and the output data V_o for both charging and discharging states at different temperatures under various battery conditions. The results are shown in Table 2. It is notable that the values of the electrical elements are considered as constant values in battery model at all different environmental and internal conditions like hysteresis effect, temperature and healthiness of battery for the equivalent state-space model. Hence, all mentioned conditions are taken into account in relation to VOC-SOC. As previously noted, nonlinear relation between VOC and SOC plays a significant role in model accuracy.

The mean value of electrical parameters for each column in table 2 is shown in table 3.

Table 1: Identified values of the electrical parameters of equivalent model

Tests conditions	R_0	R_1	R_2	C_1	C_2	α	β
Piecewise charging for new battery	0.191	0.093	0.189	1434	376	0.54	0.56
Piecewise discharging for new battery	0.197	0.087	0.193	1427	382	0.51	0.53
Continuous charging for new battery	0.2	0.092	0.187	1441	381	0.54	0.57
Continuous charging for used-battery	0.21	0.089	0.186	1430	381	0.53	0.56
Continuous discharging for used-battery	0.2	0.088	0.191	1421	371	0.5	0.54
Continuous discharging for new battery	0.21	0.087	0.195	1430	383	0.54	0.56
Piecewise charging for used-battery	0.19	0.087	0.185	1439	376	0.51	0.57
Piecewise discharging for used-battery	0.2	0.09	0.19	1432	375	0.53	0.58

Table 3: Mean values of electrical parameters

R_0	R_1	R_2	C_1	C_2	α	β
0.2	0.089	0.189	1431	378	0.52	0.56

5. Fractional State Space Model

According to Fig. 5, the state space description equations of studied system, which represent the second-order model consisting of resistors, constant phase elements and fractional order degrees are written. In this model, the open circuit voltage is considered as a nonlinear function of the SOC of the battery. SOC is also introduced as one of the state variables that should be estimated. The description of SOC based on previous researches is shown in Eq. (9):

$$\frac{dSOC}{dt} = -I_O(t)\frac{\eta}{Q_n} \tag{9}$$

Where, Q_n represents battery capacity and η is charging and discharging efficiency. They are electrochemical parameters that are measured by the manufacturer and recorded on the battery datasheet. Therefore, any changes in SOC over time will vary according to the battery current as well as these two parameters measured for each battery in the factory. By writing the description equations of the system and selecting VOC=f(SOC) as the nonlinear term connecting VOC and SOC, the state-space equations are obtained.

A sample of nonlinear state-space model is shown below:

$$\begin{Bmatrix} \frac{d^{\alpha}V_1}{dt^{\alpha}} = \frac{-V_1(t)}{R_1C_1} + \frac{I_T(t)}{C_1} \\ \frac{d^{\beta}V_2}{dt^{\beta}} = \frac{-V_2(t)}{R_2C_2} + \frac{I_T(t)}{C_2} \\ \frac{dSOC}{dt} = -\frac{\eta}{Q_n}I_T(t) \end{Bmatrix} \tag{10}$$

$$Y(t) = V_T(t) = -V_1(t) - V_2(t) + VOC(SOC) - R_0 I_T(t) \tag{11}$$

The battery voltage output will be the same as the y. Unknown parameters to be identified include *R*0, R1, R2, C1, C2, α, and. Although in many similar researches, the system is considered commensurate, in this research due to the independence of CPEs from each other, the equations are written in an incommensurate form. Therefore, there is no relationship between alpha and beta, and each CPE branch describes one of the system's dynamics:

$$\begin{Bmatrix} \dot{x} = Ax + Bu \\ y = Cx + f(SOC) + Du \end{Bmatrix} \tag{12}$$

$$X(t) = \begin{bmatrix} V_1(t) & V_2(t) & SOC(t) \end{bmatrix}^T,\ U(t) = I_T(t) \tag{13}$$

$$A = \begin{bmatrix} \frac{-1}{R_1C_1} & 0 & 0 \\ 0 & \frac{-1}{R_2C_2} & 0 \\ 0 & 0 & 0 \end{bmatrix}, B = \begin{bmatrix} \frac{1}{C_1} \\ \frac{1}{C_2} \\ \frac{-\eta}{Q_n} \end{bmatrix}, \tag{14}$$

$$C = \begin{bmatrix} -1 & -1 & d_1 \end{bmatrix}, D = -R_0$$

As seen in eq. 11, VOC must be determined according to SOC as the third state variable and substituting to state space model. In next section, based on different situation, VOC function will generated and put in look-up table due to employ in non-linear fractional order model of battery.

4.3. Determining VOC according to SOC

Curve fitting was implemented to find the relation between VOC and SOC, as a nonlinear term in state-space equations. So, the values estimation of electrical parameters is the key to obtain the nonlinear state-space model of equivalent electrical circuit model with acceptable accuracy, which was done in the previous section. The SOC values were measured using the ampere hour counting method. Then the values of VOC corresponding to SOC gathered from real tests are displayed in Fig. 5.

A polynomial curve was fitted to the SOC-VOC data, which led to a mathematical polynomial equation describing the nonlinear behavior represented as follows. To increase the accuracy, the SOC

value range of 5-95% has been considered for the curve fitting.

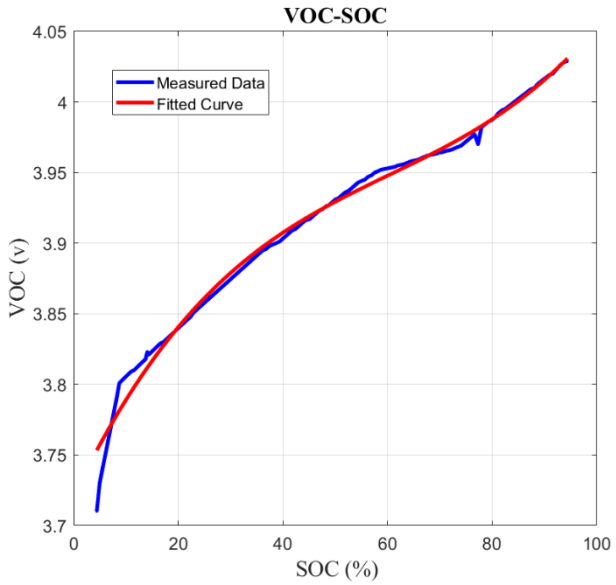

Fig. 17. Fitted curve for the VOC-SOC of new battery discharging

As shown in Figs. 17-18, two samples of VOC-SOC curves are presented. The figures also display the plots of curves fitted based on the estimated polynomial.

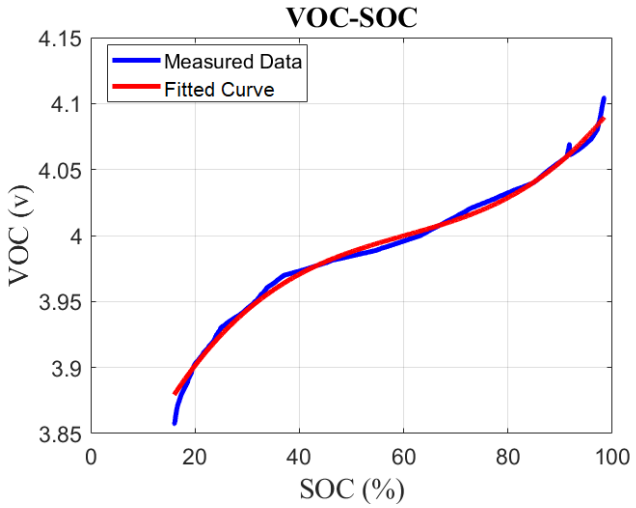

Fig. 18. Fitted curve for VOC-SOC of new battery charging

According to the experiments and analysis done during this research, four states of charging and discharging mode for the new and used battery are presented in the following equations, respectively:

New battery charging:

$$VOC = 8.312\times10^{-7}SOC^{3} - 1.498\times10^{-4}SOC^{2} + 1.012\times10^{-2}SOC + 3.752 \quad (15)$$

New battery discharging:

$$VOC = 5.436\times10^{-7}SOC^{3} - 9.842\times10^{-5}SOC^{2} + 7.729\times10^{-3}SOC + 3.721 \quad (16)$$

Used battery charging:

$$VOC = 5.03\times10^{-7}SOC^{3} - 1.035\times10^{-4}SOC^{2} + 8.715\times10^{-3}SOC + 3.725 \quad (17)$$

Used battery discharging:

$$VOC = 5.632\times10^{-7}SOC^{3} - 1.308\times10^{-4}SOC^{2} + 0.011SOC + 3.705 \quad (18)$$

A sample form of battery identification look-up table is presented in Table 4. it is worth noting that, to increase the accuracy of battery modelling, much more conditions can be considered.

Table 4: Sample format of battery modeling lookup table

Condition	Charge/discharge	Life cycle	Temperature
1	Charge	0-200	0-15
2	Discharge		
3	Charge	200-500	
4	Discharge		
5	Charge	0-200	15-30
6	Discharge		
7	Charge	200-500	
8	discharge		

It is worth mentioning that optimal temperature for high performance of lithium-ion batteries is in the range of 15-35 0C. By increasing or decreasing the temperature above or below this range, the battery's performance is deteriorated [44]. As mentioned before, in order to establish an accurate model for battery, several tests are implemented on a battery in the factory; then a look-up table is gathered. Then, based on the look-up table, the equivalent state space is determined and switched to a new model for each environmental and internal condition. Based on the gathered look up table (table 4) and assuming a new battery in charging mode and 25 C ambient temperature, the equivalent state space model is written as follows:

$$\begin{bmatrix} \frac{d^{\alpha}X_1}{dt^{\alpha}} \\ \frac{d^{\beta}X_2}{dt^{\beta}} \\ \frac{dX_3}{dt} \end{bmatrix} = \begin{bmatrix} \frac{-1}{127.36} & 0 & 0 \\ 0 & \frac{-1}{71.44} & 0 \\ 0 & 0 & 0 \end{bmatrix} \begin{bmatrix} X_1 \\ X_2 \\ X_3 \end{bmatrix} + \begin{bmatrix} \frac{1}{1431} \\ \frac{1}{378} \\ \frac{-0.95}{2} \end{bmatrix} U(t) \quad (19)$$

$$y = -X_1 - X_2 + 8.312\times10^{-7}X_3^{3} - 1.498\times10^{-4}X_3^{2} + 1.012\times10^{-2}X_3 + 3.75 - 0.2U(t)$$

6. Validation

Ultimately, by applying new inputs to the state-space equations describing the equivalent electrical circuit and comparing its output to the actual data, accuracy of the proposed model is assessed.

To validate the obtained model, a test input/ output data was employed, which has not been not used in the training steps, and by applying the input to the identified system, measuring y and comparing the values with the actual measurements, validity of obtained system was examined.

In Fig. 19, battery current with negative values, indicating the charging mode, is applied to test the battery.

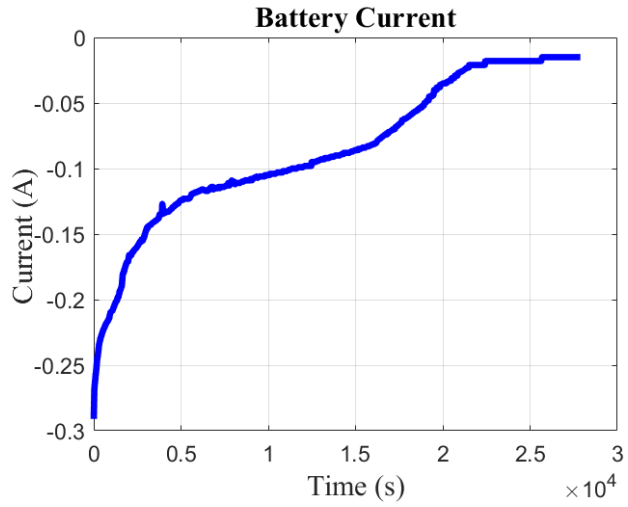

Fig. 19. Real battery charge current for new battery

Test input is employed to the proposed model and computed output is achieved. Then the real output, which is gathered by measuring the terminal voltage and current of the battery, is plotted with the simulated output in the same figure (See Fig. 20).

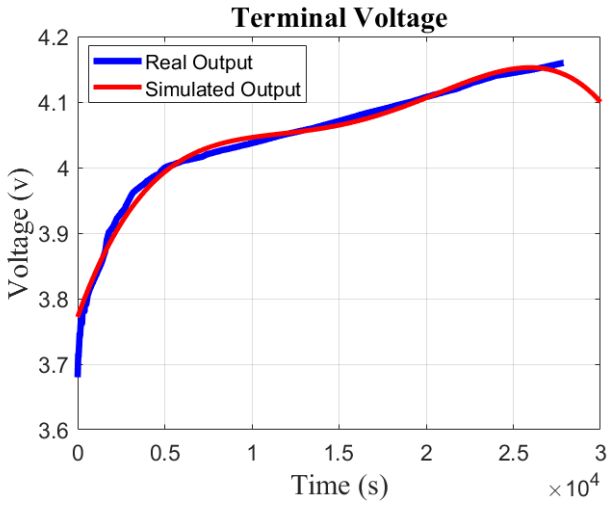

Fig. 20. Simulated and real output curves

Based on the analysis done on the proposed model of battery and validating it on the achieved equivalent state space model, precise performance of the model is proved.

7. Conclusion

One of the common approaches of battery modelling for estimating the state of charge in lithium-ion batteries under environmental and internal conditions (such as hysteresis, temperature and aging) is through adaptive methods. So, real-time modelling approaches, identification of model parameters, and state estimation or control of battery are performed instantaneously. However, in this research, which is being implemented on a solar-powered smart lighting device, instead of performing continuous battery modelling and complex computations, a different approach has been employed. Before installing the battery in the devices, there is a pre-test stage leading to generating a look-up table that associates the appropriate battery model and parameters with the corresponding SOC values. Consequently, during the actual operation of device, the required battery model and parameters are simply looked up from the pre-generated table, without the need for intensive real-time calculations. This significantly reduces the computational overhead compared to adaptive models.

The advantage of this approach is that it trades off some model accuracy for significantly lower computational requirements, which is suitable for resource-constrained embedded systems like solar-power smart lighting devices. By performing the battery characterization upfront, reasonably precise SOC estimation can be achieved.

In conclusion, it is worth mentioning that the most significant research gap addressed in this study is the development of a device capable of measuring SOC of a battery with minimal computations and high accuracy. As mentioned earlier, there is no physical device currently available to perform this task. Most of the devices introduced primarily estimate this parameter with a high computational load. It is also essential to note that detailed testing of the battery to be used must be conducted at the factory before installation in the equipment that utilizes the battery. A look-up table specific to that particular battery should also be prepared. It is also worth mentioning that by conducting precises tests, all conditions affecting the battery in its operational state are taken into account. For instance, all battery dynamics will also be reflected in the look-up table based on these detailed tests. Moreover, in most battery-powered equipment, the dynamics are generally not fast, and SOC typicaly changes slowly and gradually, without causing rapid fluctuation in the battery. Nevertheless, the fastest dynamics are also considered during the initial testing.

References

[1] B. Wang, Z. Liu, S. E. Li, S. J. Moura, and H. Peng, "State-of-charge estimation for lithium-ion batteries based on a nonlinear fractional model," *IEEE Transactions on Control Systems Technology*, vol. 25, pp. 3-11, 2016.

[2] S. Dey, "Estimation and diagnostics of lithium-ion batteries," *A Dissertation Presented*, 2015.

[3] K. S. Mawonou, A. Eddahech, D. Dumur, D. Beauvois, and E. Godoy, "Improved state of charge estimation for Li-ion batteries using fractional order extended Kalman filter," *Journal of Power Sources*, vol. 435, p. 226710, 2019.

[4] R. Divya, K. Karunanithi, S. Ramesh, and S. Raja, "A hybrid multilayerperceptron-extremegradientboost approach for precise state of charge and state of health assessment," *e-Prime-Advances in Electrical Engineering, Electronics and Energy*, vol. 8, p. 100591, 2024.

[5] M. Alam and K. Kumar, "Power Management Scheme Based on Aging Factor of Battery Storage Systems for Electric Vehicles," *e-Prime-Advances in Electrical Engineering, Electronics and Energy*, vol. 9, p. 100710, 2024.

[6] Y. Xu, M. Hu, A. Zhou, Y. Li, S. Li, C. Fu, *et al.*, "State of charge estimation for lithium-ion batteries based on adaptive dual Kalman filter," *Applied Mathematical Modelling*, vol. 77, pp. 1255-1272, 2020.

[7] J. Hidalgo-Reyes, J. Gómez-Aguilar, V. Alvarado-Martínez, M. López-López, and R. Escobar-Jimenez, "Battery state-of-charge

estimation using fractional extended Kalman filter with Mittag-Leffler memory," *Alexandria Engineering Journal*, vol. 59, pp. 1919-1929, 2020.

[8] J. Sabatier, F. Guillemard, L. Lavigne, A. Noury, M. Merveillaut, and J. M. Francico, "Fractional models of lithium-ion batteries with application to state of charge and ageing estimation," in *Informatics in Control, Automation and Robotics: 13th International Conference, ICINCO 2016 Lisbon, Portugal, 29-31 July, 2016*, 2018, pp. 55-72.

[9] H. Rahimi-Eichi, *Online adaptive battery parameters identification, and state of charge (soc) and state of health (soh) co-estimation*: North Carolina State University, 2014.

[10] N. V. Thuy and N. Van Chi, "State of charge estimation for lithium-ion battery using sigma-point Kalman filters based on the second order equivalent circuit model," in *Advances in Engineering Research and Application: Proceedings of the International Conference on Engineering Research and Applications, ICERA 2019*, 2020, pp. 664-678.

[11] J. Zeng, S. Wang, W. Cao, M. Zhang, C. Fernandez, and J. M. Guerrero, "Improved fractional-order hysteresis-equivalent circuit modeling for the online adaptive high-precision state of charge prediction of urban-electric-bus lithium-ion batteries," *International Journal of Circuit Theory and Applications*, vol. 52, pp. 420-438, 2024.

[12] P. Takyi-Aninakwa, S. Wang, G. Liu, A. N. Bage, F. Masahudu, and J. M. Guerrero, "An enhanced lithium-ion battery state-of-charge estimation method using long short-term memory with an adaptive state update filter incorporating battery parameters," *Engineering Applications of Artificial Intelligence*, vol. 132, p. 107946, 2024.

[13] X. Fan, H. Feng, X. Yun, C. Wang, and X. Zhang, "SOC estimation for lithium-ion battery based on AGA-optimized AUKF," *Journal of Energy Storage*, vol. 75, p. 109689, 2024.

[14] X. Zhang, L. Duan, Q. Gong, Y. Wang, and H. Song, "State of charge estimation for lithium-ion battery based on adaptive extended Kalman filter with improved residual covariance matrix estimator," *Journal of Power Sources*, vol. 589, p. 233758, 2024.

[15] D. Valério and J. S. Da Costa, "Introduction to single-input, single-output fractional control," *IET control theory & applications*, vol. 5, pp. 1033-1057, 2011.

[16] B. Xia, X. Zhao, R. De Callafon, H. Garnier, T. Nguyen, and C. Mi, "Accurate Lithium-ion battery parameter estimation with continuous-time system identification methods," *Applied energy*, vol. 179, pp. 426-436, 2016.

[17] C.-Y. Hsu, Y. Ajaj, G. K. Ghadir, H. M. Al-Tmimi, Z. K. Alani, A. A. Almulla, *et al.*, "Rechargeable Batteries for Energy Storage: A review," *e-Prime-Advances in Electrical Engineering, Electronics and Energy*, p. 100510, 2024.

[18] W. Merrouche, F. Harrou, B. Taghezouit, and Y. Sun, "Improved lithium-ion battery health prediction with data-based approach," *e-Prime-Advances in Electrical Engineering, Electronics and Energy*, vol. 7, p. 100457, 2024.

[19] Y. Tao, "State of Charge Estimation of Lithium-ion Batteries," 2017.

[20] Y. Xiao, *Online state of charge and temperature distribution monitoring in batteries for automotive applications*: The University of Texas at Dallas, 2015.

[21] A. Singh, K. Pal, and C. Vishwakarma, "State of charge estimation techniques of Li-ion battery of electric vehicles," *e-Prime-Advances in Electrical Engineering, Electronics and Energy*, vol. 6, p. 100328, 2023.

[22] S. J. Moura, J. L. Stein, and H. K. Fathy, "Battery-health conscious power management in plug-in hybrid electric vehicles via electrochemical modeling and stochastic control," *IEEE Transactions on Control Systems Technology*, vol. 21, pp. 679-694, 2012.

[23] B. Pattipati, B. Balasingam, G. Avvari, K. R. Pattipati, and Y. Bar-Shalom, "Open circuit voltage characterization of lithium-ion batteries," *Journal of Power Sources*, vol. 269, pp. 317-333, 2014.

[24] S. E. Li, B. Wang, H. Peng, and X. Hu, "An electrochemistry-based impedance model for lithium-ion batteries," *Journal of Power Sources*, vol. 258, pp. 9-18, 2014.

[25] Y. Jiang, X. Zhao, A. Valibeygi, and R. A. De Callafon, "Dynamic prediction of power storage and delivery by data-based fractional differential models of a lithium iron phosphate battery," *Energies*, vol. 9, p. 590, 2016.

[26] I.-S. Kim, "A technique for estimating the state of health of lithium batteries through a dual-sliding-mode observer," *IEEE Transactions on power electronics*, vol. 25, pp. 1013-1022, 2009.

[27] A. Moshar Movahhed, H. Toossian Shandiz, and S. K. Hoseini Sani, "Fractional modeling and analysis of buck converter in CCM mode peration," *Journal of AI and Data Mining*, vol. 5, pp. 327-335, 2017.

[28] A. M. Movahed, H. T. Shandiz, and S. K. Hosseini Sani, "Comparison of fractional order modelling and integer order modelling of fractional order buck converter in continuous condition mode operation," *Advances in Electrical and Electronic Engineering*, vol. 14, pp. 531-542, 2016.

[29] C. A. Monje, Y. Chen, B. M. Vinagre, D. Xue, and V. Feliu-Batlle, *Fractional-order systems and controls: fundamentals and applications*: Springer Science & Business Media, 2010.

[30] A. K. Mahmood and B. F. Mohammed, "Design optimal fractional order PID controller utilizing particle swarm optimization algorithm and discretization method," *International Journal of Emerging Science and Engineering*, vol. 1, pp. 87-92, 2013.

[31] A. Oustaloup, F. Levron, B. Mathieu, and F. M. Nanot, "Frequency-band complex noninteger differentiator: characterization and synthesis," *IEEE Transactions on Circuits and Systems I: Fundamental Theory and Applications*, vol. 47, pp. 25-39, 2000.

[32] Y. Hu and S. Yurkovich, "Linear parameter varying battery model identification using subspace methods," *Journal of Power Sources*, vol. 196, pp. 2913-2923, 2011.

[33] J. Remmlinger, M. Buchholz, M. Meiler, P. Bernreuter, and K. Dietmayer, "State-of-health monitoring of lithium-ion batteries in electric vehicles by on-board internal resistance estimation," *Journal of power sources*, vol. 196, pp. 5357-5363, 2011.

[34] S. Lee, J. Kim, J. Lee, and B. H. Cho, "State-of-charge and capacity estimation of lithium-ion battery using a new open-circuit voltage versus state-of-charge," *Journal of power sources*, vol. 185, pp. 1367-1373, 2008.

[35] G. P. Rao and H. Unbehauen, "Identification of continuous-time systems," *IEE Proceedings-Control theory and applications*, vol. 153, pp. 185-220, 2006.

[36] J. Peng, J. Luo, H. He, and B. Lu, "An improved state of charge estimation method based on cubature Kalman filter for lithium-ion batteries," *Applied energy*, vol. 253, p. 113520, 2019.

[37] G. L. Plett, "Extended Kalman filtering for battery management systems of LiPB-based HEV battery packs: Part 3. State and parameter estimation," *Journal of Power sources*, vol. 134, pp. 277-292, 2004.

[38] H. Garnier, M. Mensler, and A. Richard, "Continuous-time model identification from sampled data: implementation issues and performance evaluation," *International journal of Control*, vol. 76, pp. 1337-1357, 2003.

[39] D. Gandolfo, A. Brandao, D. Patiño, and M. Molina, "Dynamic model of lithium polymer battery–load resistor method for

electric parameters identification," *Journal of the Energy Institute*, vol. 88, pp. 470-479, 2015.

[40] M. Eckert, L. Kölsch, and S. Hohmann, "Fractional algebraic identification of the distribution of relaxation times of battery cells," in *2015 54th IEEE Conference on Decision and Control (CDC)*, 2015, pp. 2101-2108.

[41] Y. Jiang, B. Xia, X. Zhao, T. Nguyen, C. Mi, and R. A. de Callafon, "Identification of fractional differential models for lithium-ion polymer battery dynamics," *IFAC-PapersOnLine*, vol. 50, pp. 405-410, 2017.

[42] S. Liu, X. Dong, and Y. Zhang, "A new state of charge estimation method for lithium-ion battery based on the fractional order model," *IEEE Access*, vol. 7, pp. 122949-122954, 2019.

[43] X. Hu, S. Li, and H. Peng, "A comparative study of equivalent circuit models for Li-ion batteries," *Journal of Power Sources*, vol. 198, pp. 359-367, 2012.

[44] G. A. P. Rao and S. S. Kumar, "A Review of Integrated Battery Thermal Management Systems for Lithium-Ion Batteries of Electric Vehicles," *e-Prime-Advances in Electrical Engineering, Electronics and Energy*, p. 100526, 2024.